Reports of CFRL (*Cold Fusion Research Laboratory*) **12-3**, 1 – 16 (April, 2012)

The Cold Fusion Phenomenon in Hydrogen-graphites

Hideo Kozima* and Masahito Tada**
*Cold Fusion Research Laboratory, 597-16 Yatsu, Aoi, Shizuoka, 421-1202 Japan
**Institute of Natural Medicine, Toyama University, 2630 Toyama, 930-0194 Japan

*This is an extended version of the paper with the same title published in *Proc. JCF12* (Kobe, Japan, December 17 – 18, 2011), pp. 77 – 92 (2012) and posted at JCF website: http://jcfrs.org/file/jcf12-proceedings.pdf

Abstract

The cold fusion phenomenon (CFP) observed in solid materials with specific compositions (CF-materials) in open, non-equilibrium conditions has been consistently explained by a model assuming existence of neutrons in the materials. The essential factor of the material where realized the CFP is the interlaced superlattices of a host atom and a hydrogen isotope (protium and/or deuterium); one example of the first is Ni-H and another of the second is Pd-D. An exceptional example is XLPE (cross-linked polyethylene) in which a carbon lattice and protium lattice are interlaced according to its special structure.

In addition to the systems described above, there are several experimental data on the nuclear transmutation in carbon systems. In these experiments, a lot of iron is produced in addition to other elements such as Ca, Si, Cr, Mn, Co, Ni, Cu and Zn when carbon (graphite) is used as electrodes for arcing in water and in air. Furthermore, it is shown that the isotopic ratio of the generated iron is the same to the natural one. These elements found in the experiments exist abundant in nature as we had pointed out in relation to one of the statistical laws in the CFP, the stability effect of nuclear transmutation products, as shown in Fig. 2.11 of our book *The Science of the Cold Fusion Phenomenon* (2003, ISBN 0-080-45110-1)

On the other hand, it is well known that graphite absorbs hydrogen isotopes very much as to be nominated as a reservoir of hydrogen. In our previous papers, the formation of neutron drops in the cf-matter due to the interaction between carbon sublattice and proton sublattice is used for the explanation of nuclear transmutations in XLPE. This mechanism suggests that a similar interaction may exist in the hydrogen-graphite where the carbon sublattice of graphite interacts with the proton sublattice interlaced with the former.

Then, the neutron drops in the cf-matter formed by the interaction between the interlaced sublattices facilitate the generation of new elements in hydrogen-graphite at a condition of room temperature. The generated elements have, as the stability effect of nuclear transmutation shows, similar characteristics to

elements generated in celestial conditions. The experimental results obtained in the carbon arcing in water and in air show a possible application of CFP in hydrogen-graphite to eliminate hazardous nuclear waste by nuclear transmutations and to generate excess energy economically.

1. Introduction

The cold fusion phenomenon (CFP) discovered more than twenty years ago [1.1, 1.2] is composed of complex features with various fields of its occurrence and various products composed of excess energy exceeding those expected from possible chemical and physical processes and of new elements or nuclides only expected from nuclear reactions.

At first, some of these products observed by the pioneers of this field have been assumed to be results of nuclear fusion reactions in the material composed of transition metals, Ti, Ni, or Pd, and hydrogen isotopes, H and/or D. The phenomenon has been called “cold fusion” irrespective of inconsistency between the expectation based on the assumed fusion reactions between hydrogen isotopes and the experimental results.

As the increase of experimental data sets in various materials with large variety of composition has shown inadequacy of the use of the name “cold fusion” to express this new field, we proposed a name “cold fusion phenomenon (CFP)” keeping the original naming and considering our ignorance about the necessary and sufficient conditions for this phenomenon. We use this name throughout this paper also together with its abbreviated form CFP.

As we know at present [1.3, 1.4], the cold fusion phenomenon (CFP) encompasses a large variety of materials where occurs the CFP (CF materials) and of products only understandable by the occurrence of nuclear reactions (products of nuclear transmutations) accompanying excess energy.

Not considering the transition metal-hydrogen isotope systems, the most extensively investigated CF materials, there is very interesting CF materials composed of carbon and hydrogen isotopes. The one extensively investigated is the cross-linked polyethylene (XLPE) where detected generation of new elements in relation to the appearance of the so-called water trees. The data has been investigated and given a consistent explanation based on our model [1.5].

In addition to the data sets of XLPE, there are several data sets of nuclear transmutations in CF materials composed of carbon (graphite) and hydrogen. Due to the fragility of the material, the detailed investigation of the nuclear transmutation in these materials has been in its infantile stage. In this paper, we will take up experimental data

sets obtained in this difficult material for its interesting properties and also its hopeful applications along our line of investigation successfully applied to XLPE and also to other CF materials [1.3, 1.5, 1.6]

2. Experimental Facts

Carbon is an element popular in our daily life. It is also used in our technology almost everywhere especially in electronics. Recently, graphite is noticed for its high ability to include a lot of hydrogen isotopes in relation to the demand for hydrogen as a fuel. Another property of graphite eagerly investigated is its use for walls of fusion apparatuses.

Unfortunately, the pioneering works on the graphite as a CF material revealing its ability to generate nuclear transmutation and accompanying excess energy is looked over due perhaps to the fragility of graphite causing poor reproducibility even if we expect a qualitative one for the CFP in general.

We survey experimental data sets of the CFP observed in materials including carbon (graphite) and necessarily hydrogen in this section.

2.1 Nuclear Products of Carbon Arcs in Water and in Air

The experimental data sets reporting nuclear transmutations in CF materials composed of carbon (graphite) and hydrogen have been started with the arc discharge in water with carbon (C) cathode and C or other metals. In these experiments, excess energy has been out of consideration due to their experimental conditions.

2.1.1 R. Sundaresan and J. O'M. Bockris

R. Sundaresan and J. O'M. Bockris [2.1] observed generation of iron (F) by carbon arc in highly purified water in the presence of oxygen. The amount of the generated iron increased with the time of discharge as shown in Fig. 2.1.

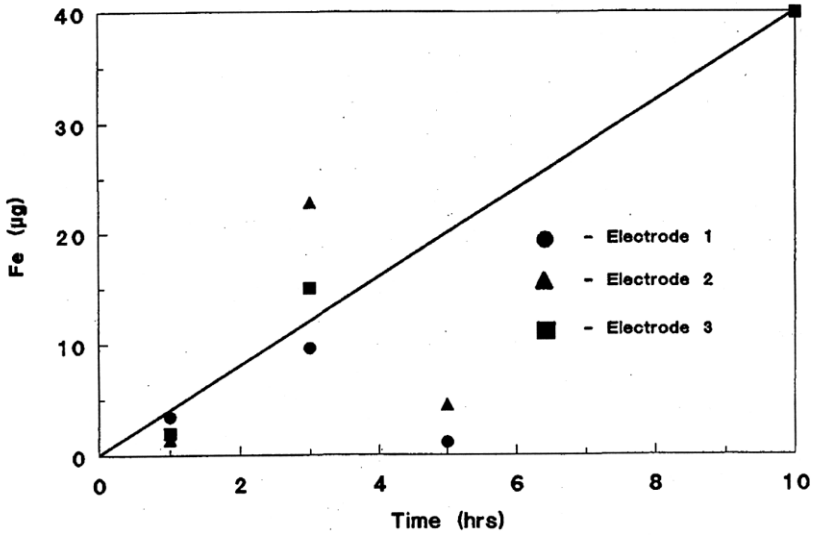

Fig. 2.1 Effect of time of electrolysis on the formation of iron (Sundaresan et al. Fig. 2 [2.1])

2.1.2 M. Singh, M.D. Saksena, V.S. Dixit and V.B. Kartha,

Singh et al. [2.2] used DC arc between ultrapure graphite electrodes dipped in ultrapure water. The graphite residue collected at the bottom of the water trough was analyzed for iron content to show that the iron content in the graphite residue was fairly high, depending on the duration of the arcing. The experiment was repeated initially six times, and the results showed large variations in iron content [50 to 2000 ppm] in the carbon residue.

The iron in the carbon residue was also analyzed mass spectrometrically for the abundance of its various isotopes, and the results were more or less the same as that of natural iron as shown in Table 2.1. Besides iron (Fe), the presence of other elements like silicon (Si), nickel (Ni), aluminum (Al), and chromium (Cr) was also determined in the carbon residue, and it was found that the variation of their concentrations followed the same pattern as that of iron.

Table 2.1 Mass spectrometric analysis results of the iron recovered from the graphite residue in the carbon arc in water experiments along with the analysis of natural iron (Spec pure) [2.2, Table II].

Experiment Number	Atom Ratios of Iron Isotopes		
	$^{54}Fe/^{56}Fe$	$^{57}Fe/^{56}Fe$	$^{58}Fe/^{56}Fe$
3	[a]	0.0231 ± 0.0007	[a]
Natural iron (Spec pure)	0.0636 ± 0.0005	0.0230 ± 0.0002	0.00310 ± 0.00004
4	[a]	0.0230 ± 0.0002	[a]
Natural iron (Spec pure)	0.0635 ± 0.0005	0.0233 ± 0.0002	0.00308 ± 0.00004
5	0.0635 ± 0.0010	0.0232 ± 0.0002	[a]
Natural iron (Spec pure)	0.0638 ± 0.0005	0.0233 ± 0.0002	0.00310 ± 0.00004

[a]In the sample, because of isobaric interference of $^{54}Cr^+$ and $^{58}Ni^+$, the respective iron isotope results of $^{54}Fe/^{56}Fe$ and $^{58}Fe/^{56}Fe$ could not be reported.

2.1.3 I. Ogura, I. Awata, T. Takigawa, K. Nakamura, O. Horibe and T. Koga,

In the experiments by Ogura et al. [2.3], arc discharge was carried out in a water phase (distilled H_2O was used) with a DC discharge voltage of 25 V (110 V for the case (2) below). From analysis of water used for the carbon arc discharge, increases in quantity of Ca, Fe, and other several elements were recognized. When silicon or metal sticks were used for the counter electrode, the content of Ca was distinctly increased with the former. The amount of the generated element increases with the discharge time.

In the arc discharges, carbon (C) is used as the cathode, and as the anode (1) $_6$C, (2) $_{14}$Si, (3) $_{23}$V, (4) $_{22}$Ti, (5) $_{27}$Co, or (6) $_{28}$Ni is used. Generation of new elements in these cases is (1) Ca, V, Cr, Ni (by PIXE analysis) (2) Remarkable increase of Ca on the anode, (3) Ca, Cr, Fe, Cu (by PIXE analysis) (4) $_{23}$V, (5) $_{28}$Ni, and (6) $_{29}$Cu. In the cases (4) – (6), it is noticed that the generated elements have one more large proton numbers than the anode metals; $_{22}$Ti $\rightarrow_{23}$V , $_{27}$Co $\rightarrow_{28}$Ni, and $_{28}$Ni$\rightarrow_{29}$Cu.

2.1.4 T. Hanawa

Hanawa [2.4] made experiments of carbon arc in (1) pure water and (2) aqueous electrolyte with Li_2CO_3 0.05 mol/*l* and (3) one with Na_2CO_3 0.05 mol/*l*. He observed Ca, Cr, Mn, Fe, Co, Ni, Cu, and Zn in cases (1), (2) and (3) in carbon residue. In the cases (2) and (3), there are no Ca, Co and Cu on the electrodes. In the case (3), there are a lot of metals on the anode.

Recently Esko [2.5] made an experiment similar to those introduced above. Non-metallic graphite or silicon powders (scientific grade 99.999% pure) are placed in a pure (99.999%) graphite crucible. The powders are charged with 36 V of direct current through a pure (99.999%) graphite rod. The crucible is connected to the negative pole, the rod to the positive pole of a power pack consisting of three 12 V solar charged batteries.

The powders display apparent magnetic activity following the above treatment. Moreover, magnetic activity remains in the powders six months after treatment, suggesting the effect is permanent. Treated graphite shows the presence of magnetic iron at a level of up to 1.6% by weight. A typical analysis sample (ICP analysis by New Hampshire Materials Laboratory,
August 9, 2007) shows the appearance of metals Si (10.500), Mg (1800), Fe (4700), Cu (4200), Al (7800), Ti (440), S (580) and K (1000 ppm) in treated graphite.

In addition to changes in the composition of the graphite power used in the tests, changes have been noted in the pure graphite rods used in the experiments. In a study conducted in October 2007, a shiny metallic "bubble" appeared on the striking surface of the rod. Upon analysis, the rod was found to contain the following metals Sc (35), Fe (640), Co (160) and Ni (1120 ppm).

2.2 Electrolysis with Charcoal Cathode with Light and Heavy Waters

A somewhat different experiment was performed by R. Takahashi [2.6].

2.2.1 R. Takahashi

He used charcoal cathode in electrolysis with electrolytes of 0.25N alkali hydroxides (LiOH, NaOH, KOH, RbOH and CsOH) in D_2O, $D_2O + H_2O$, and H_2O. The input power was less than 4 W. Colorization of electrolyte liquids is observed with excess heat generation showing synthesis of substance by the electrolysis when D_2O or D_2O (0.75) + H_2O (0.25) is used. Maximum excess heat was observed for the electrolyte of LiOH in D_2O (0.75) + H_2O (0.25) with an input power 2.5 W. He concluded that charcoal tends to form chemical compounds in the electrolysis and from this reason the fusion between deuterons, the cause of the excess heat, is poor.

2.3Characteristics of the Experimental Results

The experimental data obtained in the carbon arc experiments are destined by the statistical nature that is a common characteristic to nuclear reactions such as the statistical law governing the alpha decay of radium $^{226}_{88}Ra \rightarrow {}^{222}_{86}Rn$ ($\tau_{1/2} = 1.6\times10^3$ y). Therefore, we will look at the data as a total not individually.

2.3.1 Elements observed in Carbon Arcing Experiments in Water

(1) Detection of New Elements

The experimental data introduced in Section 2.2 are summarized as follows;
Sundaresan and Bockris; Fe
Singh et al.; Si, Ni, Al, Cr, Mn, Fe (and ratios $^{54}Fe/^{56}Fe$, $^{57}Fe/^{56}Fe$, $^{58}Fe/^{56}Fe$)

Ogura et al.; Ca, V, Cr, Fe, Ni, Cu
Hanawa; Ca, Cr, Mn, Fe, Co, Ni, Cu, Zn
Esko; Si, Mg, Fe, Co, Ni, Cu, Al, Ti, S, K

As a whole, we can list up the generated elements as follows according to their proton numbers with frequency in a parenthesis after the symbol.
$_{12}$Mg (1), $_{13}$**Al (2),** $_{14}$**Si (2),** $_{16}$S (1), $_{19}$K (1), $_{20}$**Ca (2),** $_{22}$Ti (1), $_{24}$**Cr (3),** $_{25}$**Mn (2),** $_{26}$**Fe (5),** $_{27}$**Co (2),** $_{28}$**Ni (4),** $_{29}$**Cu (3),** $_{30}$Zn (1).

The elements observed more than twice are marked by bold letters.

(2) Determination of Isotopic Ratios

The isotopic ratios ^{54}Fe/^{56}Fe, ^{57}Fe/^{56}Fe, ^{58}Fe/^{56}Fe detected by Singh et al. are not different from natural ones.

(3) Excess heat

The excess heat and unknown elements in the liquid are observed in the electrolytic experiment by R. Takahashi [2.6]. In relation to this experiment with charcoal cathodes, we would like to point out a characteristic of the charcoal. Charcoal has micro-channels built in biologically. This characteristic of the natural regular array of carbon corresponds to the graphite lattice in the carbon arc experiments and has close relation to biological nuclear transmutations as discussed several times by now, e.g. in our paper [2.8] and book [2.9, Section 10.1].

We have discussed possible formation of regular arrangement of physiological cells to realize nuclear transmutations in biological systems. If the CFP is confirmed in charcoal systems and graphites, possibility of biological nuclear transmutation will have a strong support.

2.4 Comparison of the Experimental Data with other Data obtained in the CFP

The first law of the CFP found by comparison of the data in the CFP [1.3] and the data obtained in the Universe [2.7] says that the more natural abundance of an element is the more product of the element by nuclear transmutation in the CFP as shown in Fig. 2.2.

The peaks of the $\log_{10}H$ in Fig. 2.2 correspond to the following Z's shown in Table 2.2. It is clear that they coincide with the elements marked by bold letters observed in carbon arcing experiments except $_{25}$Mn which is not at a peak but the value is fairly

large.

Table 2.2 Peaks of $\log_{10}H$ of elements in the universe [2.7].

Z	13	14	20	24	[25]	26	28	29	30
Element	Al	Si	Ca	Cr	Mn	Fe	Ni	Cu	Zn

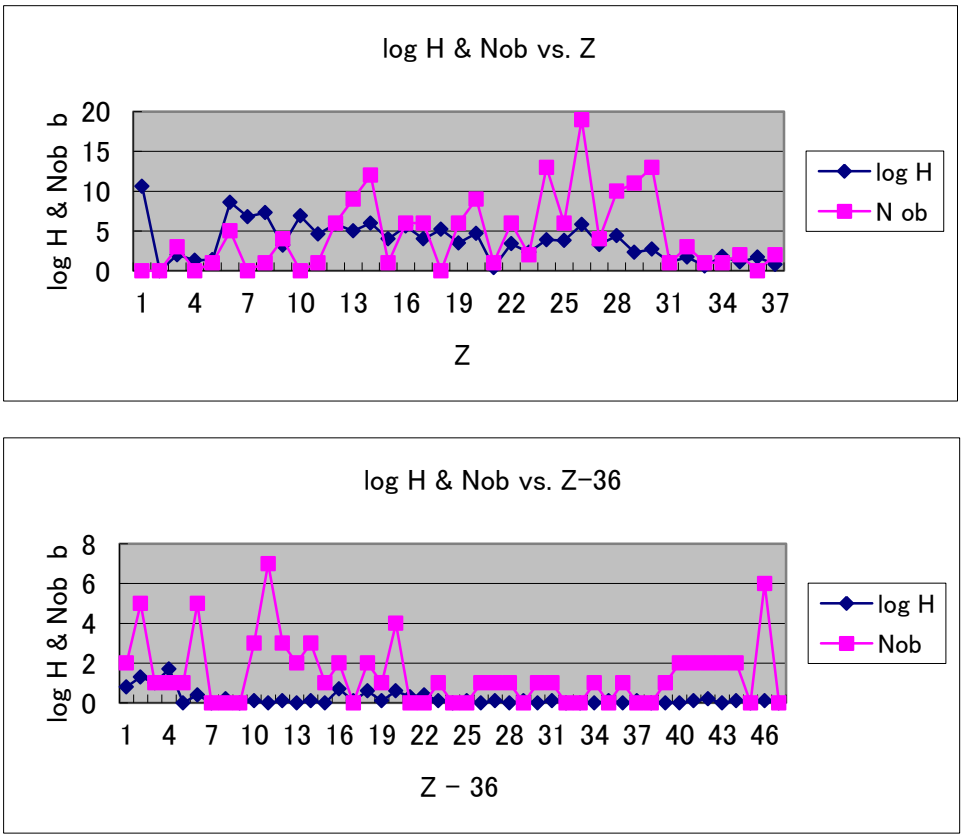

Fig. 2.2 Correspondence between the frequency N_{ob} observing elements in the CFP and the relative abundances $\log_{10}H$ of elements in the universe [2.7]; (a) (Z = 3 – 38), (b) (Z = 39 – 83) [1.3, Fig. 2.11].

Therefore, this law (the First Law of the CFP) seems applicable to the case of nuclear transmutation products in the above case of carbon arcing and tells us that the nuclear transmutation in the carbon arc is a phenomenon belonging to the same CFP as observed in the transition-metal hydrides and deuterides.

The isotopic ratios of iron nuclides observed by Singh et al. [2.2] are similar to the natural ones and is also an evidence of the replication of the nuclear reactions in the star by the nuclear transmutation in the CFP depicted in the First Law of the CFP, the

stability effects of NT in the CFP [1.3, Section 2.5.5].

3 Theoretical Approach to the Nuclear Transmutation in Hydrogen-graphites

The experimental data sets overviewed in the preceding section confirm that it is possible to apply our theory successful in the explanation of the CFP in transition-metal hydrides and deuterides to the present case.

Our theory is based on the formation of the neutron band in the CF material where occurs the CFP. The neutron band is formed by the super-nuclear interaction between lattice nuclei X's at different lattice points mediated by hydrogen isotopes Y's (H or D) at interstices when X and Y are on the interlaced sublattices of a superlattice. We examine a possibility of the neutron band formation in hydrogen-graphite using the current knowledge of carbon nuclei and graphite structure.

For the formation of the neutron band, there are three necessary conditions related to host nuclei, hydrogen isotopes and the superlattice composed of host sublattice and hydrogen sublattice.

3.1 Neutron Halo in Carbon Nuclei

Recently, many exotic nuclei with neutron halo of medium and heavy nuclei were discovered such as $^{19}_{6}$C [3.1], $^{22}_{6}$C [3.2], and $^{31}_{10}$Ne [3.3] by RIBF (RI beam factory) experiments.

The neutron halo of these carbon nuclei, $^{19}_{6}$C and $^{22}_{6}$C, is favorable for the realization of the neutron band as is discussed before [1.3, Section 3.7] in cooperation with the extended wave functions of hydrogen isotopes in graphite as shown in Section 3.3.

What kind of structure the nucleus has at the neutron drip line? This question is not solved yet. It is, however, theoretically concluded that there are few halo structures in heavy nuclei at neutron drip line [3.4]. If this conclusion is right, carbon is a favorable nucleus for the host as a CF material even if heavier nuclei that have no stable halo states in free space may become halo states by interaction with hydrogen isotopes in super-lattice. The halo states of carbon nucleus work to realize super-nuclear interaction even if the H or D lattice is not perfect to form the necessary ideal super-lattice supposed for PdD or NiH [1.3, Section 3.7].

3.2 Extended Proton Wavefunctions in Graphite

Unfortunately, there are no explicit data of proton (or deuteron) wavefunctions in

graphite crystal due perhaps to the fragility of the lattice and wide spread character of the wavefunctions. There are, however, results of simulations showing rather extended proton wavefunctions in graphene double layer (Graphene sheets stack to form graphite with an interplanar spacing of 0.335 nm) as shown in Fig. 3.1 [3.5].

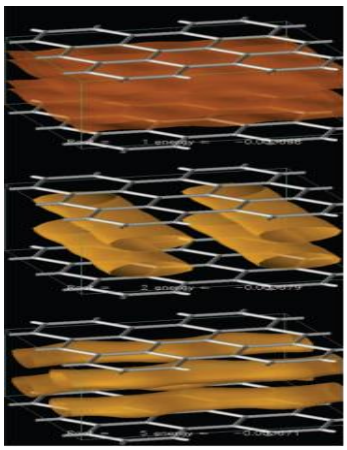

Fig. 3.1 Probability densities for selected lowest eigenstates of the translational nuclear Hamiltonian. The lowest in-phase (top to bottom: first, second, and fifthe) eigenstates for the double-layer structure are shown (d = 8Å) [3.5].

3.3 Superlattice of Carbon and Hydrogen

The structure of a graphite lattice including hydrogen isotopes is not explicitly shown due perhaps to the fragility and difficulty to obtain an ideal sample. However, there is a lot of data on the lattice structure of LiC_6 used in the lithium battery [3.6, 3.7]. The lattice structure of LiC_6 is depicted as shown in Fig. 3.2 [3.6].

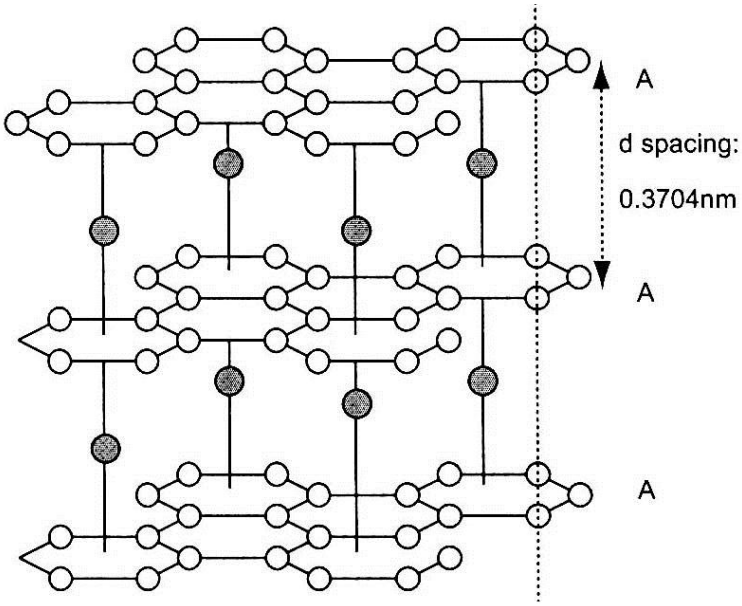

Fig. 3.2 Lattice structure of LiC_6 (○:C, ●:Li) [3.6]

We can guess the structure of HC_x by analogy with LiC_6 as follows. The protons may locate at similar interstices as Li atom in LiC_6 with more extended wavefunctions as shown in Fig. 3.1 due to the light mass of proton ^1_1H compared to ^6_3Li or ^7_3Li. Therefore, we can imagine the structure of HC_x as a superlattice composed of a carbon sublattice and another proton sublattice, the latter may be rather incomplete.

The data obtained by NMR studies support this conjecture as follows [3.8]. The NMR spectrum of $C^{nano}H_{0.96}$ is well represented by the sum of a Lorentzian and a Gaussian line, indicating two types of hydrogen coordinations. These two components may be ascribed to hydrogen in graphite interlayers and hydrogen chemisorbed at dangling bonds.

On the retention and diffusion of proton in graphite, there is a data telling us diffusion of protons in graphite lattice along the layer as shown in Fig. 3.3 [3.9]. The characteristics of retention and diffusion of hydrogen in graphite is expressed as follows; "When bombarded with energetic hydrogen ions at room temperature, graphite is observed to retain all non-reflected hydrogen until a saturation concentration is reached. At room temperature the saturation level is ~ 0.4 H/C. Further implanted hydrogen is rapidly released at virtually the implantation rate. However, some hydrogen atoms may be driven into the bulk of graphite beyond the saturated implantation layer. - - - While molecular hydrogen does not react with graphite, the chemical reaction between atomic hydrogen and graphite occurs at thermal hydrogen energies in the absence of radiation induced displacements" [3.9].

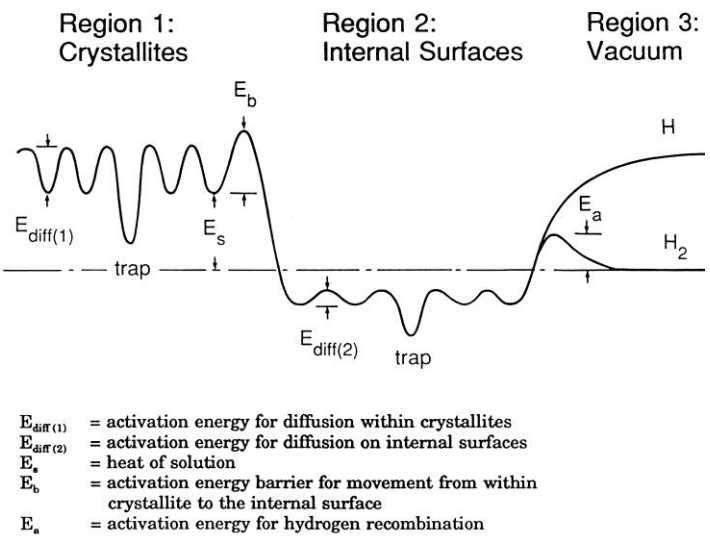

Fig. 3.3 Potential energy diagram within the bulk of graphite. Region 1 represents the crystallite

lattice, with higher activation energy and slow atom diffusion. Region 2 represents internal surfaces, with lower activation energy and fast atom diffusion. Region 3 represents the release of hydrogen into the gaseous phase (vacuum) as either atoms or molecules depending on the surface temperature. [3.9, Fig. 16]

3.4 Super-nuclear Interaction and Neutron Band Formation

It is possible to have an interaction between nuclei X($\boldsymbol{r}_i$) and X($\boldsymbol{r}_{i'}$) at different lattice points by super-nuclear interaction mediated by occluded hydrogen isotopes (H or D) at interstices ($\boldsymbol{r}_j$'s) when there is a super lattice of X and H (or D) composed of a sublattice of X and a sublattice of H (or D) [1.3, Sec. 3.7.2].

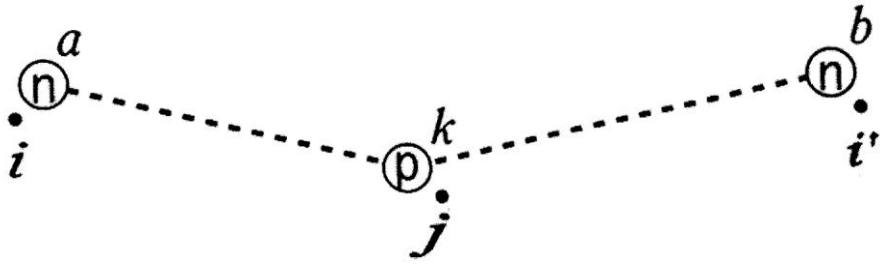

Fig. 3.4 Super-nuclear interaction between neutrons at a lattice point ***i*** and another ***i'*** mediated by a proton at an interstice ***j.***

Then, it is possible to form a neutron band by the super-nuclear interaction between lattice neutrons and there appears a high density neutron matter at a boundary region by positive interference of reflected neutron waves [1.3, Sec. 3.7.4].

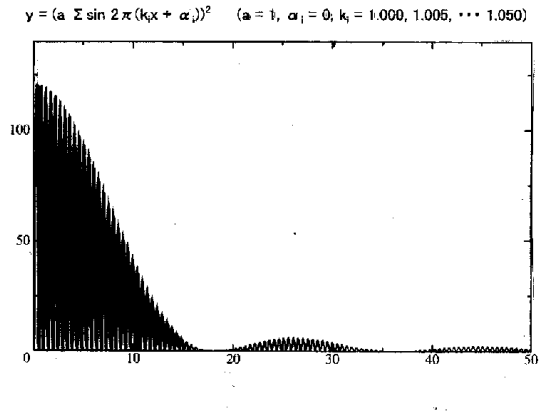

Fig. 3.5 Formation of neutron drops ${}^{A}_{Z}\Delta$ composed of Z protons and A – Z neutrons at the boundary region where neutron density becomes very high by the coherent augmentation of neutron waves reflected at the boundary [1.3, Sec. 3.7.4].

The speculation given in the previous Sections 3.1, 3.2 and 3.3 gives us a hope to expect formation of a neutron band by this super-nuclear interaction in hydrogen-graphite samples in its optimum situation with a fairly good superlattice structure. If we can expect the formation of a neutron band in a hydrogen-graphite system, there occur nuclear reactions resulting in such a CFP as that observed in the transition-metal deuterides and hydrides.

4. Discussion

We can expect two types of nuclear transmutations due to the neutron drop-nuclear interaction at the boundary region.

(1) Generation of a nucleus according to the stability effect where a rather stable neutron drop ${}^{A}_{Z}\Delta$ transforms into a nucleus ${}^{A}_{Z}X$.

$${}^{A}_{Z}\Delta \rightarrow {}^{A}_{Z}X. \quad (1)$$

(2) Generation of a nucleus ${}^{A}_{Z}X$ by an absorption of a neutron by a nucleus ${}^{A-1}_{Z}X$ and then a beta-decay of ${}^{A}_{Z}X$ to be ${}^{A}_{Z+1}X'$, i.e.

$$n + {}^{A-1}_{Z}X \rightarrow {}^{A}_{Z}X \rightarrow {}^{A}_{Z+1}X' + e^{-} + \underline{\nu}_e, \quad (2)$$

where $\underline{\nu}_e$ is an antiparticle of electron neutrino.

The generation of new elements introduced in Sections 2.1 and 2.3 reveals these two phases of the nuclear transmutation in the CFP. The frequency of detection of new elements corresponding to the First Law (stability effect) and the isotopic ratios of iron the same to the natural ones reflect the above property expressed Eq. (1).

In the experiment by Ogura et al. [2.3], they observed that the generated elements have one more large proton numbers than the anode metals suggesting following nuclear transmutations; ${}_{22}Ti \rightarrow {}_{23}V$, ${}_{27}Co \rightarrow {}_{28}Ni$, and ${}_{28}Ni \rightarrow {}_{29}Cu$. This data may be explained by the property (2) of the nuclear transmutation in the CFP expressed in Eq. (2). Actually, the nuclear data tell us that ${}^{49}_{22}Ti$ suffers the transmutation (2) to be ${}^{50}_{23}V$, ${}^{59}_{27}Co$ to be ${}^{60}_{28}Ni$, and ${}^{62}_{28}Ni$ to be ${}^{63}_{29}Cu$ by absorption of a neutron and a succeeding beta-decay.

The existence of neutron halo nuclei of carbon ${}^{19}_{6}C$ and ${}^{22}_{6}C$ is favorable for the CFP in hydrogen-graphite and also in XLPE. Recently, many exotic nuclei with neutron halo have been discovered in light and medium nuclei such as ${}^{19}_{6}C$ [3.1], ${}^{22}_{6}C$ [3.2], and ${}^{31}_{10}Ne$ [3.3] by RIBF (RI beam factory) experiments.

The neutron halo of the carbon nuclei ${}^{19}_{6}C$ and ${}^{22}_{6}C$ is favorable for the realization of the neutron band as is discussed before [1.3, Section 3.7] in cooperation with the extended wave functions of hydrogen isotopes in graphite as shown in Section 3.4.

What kind of structure the nucleus has at the neutron drip line? This question is not

solved yet. It is, however, theoretically concluded that there are few halo structures in heavy nuclei at neutron drip line [3.4]. If this conclusion is right, carbon is a favorable nucleus for the host as a CF material. The halo states of carbon nucleus work to realize super-nuclear interaction even if the superlattice composed of a carbon sublattice and H or D sublattice is not perfect. However, the fragility of graphite may give influence on the qualitative reproducibility of the CFP to make its degree less than in rather stable transition-metal hydrides and deuterides.

This may be a reason for the CFP in hydrogen-graphite despite fragility of the graphite lattice and in XLPE (crosslinked polyethylene). Furthermore, this logic can be extended to biological molecular structure where are various carbohydrate ($C_nH_{2m}O_m$) which have more or less ordered arrangements of carbon and hydrogen atoms. The data obtained by R. Takahashi [2.6] in a system composed of charcoal and deuterium might be an example of this type. Bionuclear transmutations extensively investigated by Vysotskii et al. [4.1] may essentially be understood by the same mechanism.

In the case of the NiH and PdD superlattice, the situation is a little different. Recent knowledge of the halo nucleus tells us that the formation of exotic nuclei with a large excess neutron number is limited to elements with small proton numbers *Z* in the free space. In CF materials, there is a mechanism to stabilize neutron halo nuclei with a medium *Z* value by the super-nuclear interaction mediated by hydrogen isotopes in the sublattice. Therefore, it is necessary to form a rather perfect superlattice to realize the neutron band in NiH and PdD [1.3, Section 3.7].

It should be noticed the fact that the cathodes in the carbon arc experiments become rather higher temperature as 3000 C. This fact should be closely related to the occurrence of the CFP in a hydrogen-graphite influencing the structure of the superlattice, a necessary condition for the CFP from our point of view. The self-organization of regular stable structure in non-equilibrium, open system is known in the nanotube formation [4.2]. The same mechanism may be participating in the formation of graphene (as seen in Fig. 3.1) at the surface of graphite in the carbon arc experiments.

Carbon is a hopeful material in application of the CFP and investigation of the structure giving rise to the nuclear reactions generating new elements is very important from scientific and engineering point of view.

References

1.1 M. Fleischmann, S. Pons and M. Hawkins, "Electrochemically induced Nuclear Fusion of Deuterium," *J. Electroanal. Chem*., **261**, 301 – 308 (1989).

1.2 S.E. Jones, E.P. Palmer, J.B. Czirr, D.L. Decker, G.L. Jensen, J.M. Thorne and S.E. Tayler, "Observation of Cold Nuclear Fusion in Condensed Matter," *Nature* **338**, 737 – 740 (1989)

1.3 H. Kozima, *The Science of the Cold Fusion Phenomenon*, Elsevier, 2006. ISBN-10; 0-080-45110-1

1.4 E. Storms, *The Science of Low Energy Nuclear Reactions*, World Scientific, Singapore, 2007. ISBN-10 981-270-620-8.

1.5 H. Kozima and H. Date, "Nuclear Transmutations in Polyethylene (XLPE) Films and Water Tree Generation in Them," *Proc. ICCF14* pp. 618 – 622 (2010). And also *Reports of CFRL* (Cold Fusion Research Laboratory) **8-2**, pp. 1 – 15 (2008).

1.6 H. Kozima, "Three Laws of the Cold Fusion Phenomenon and Their Physical Meaning," *Proc. JCF12* (to be published). And also *Reports of CFRL* (Cold Fusion Research Laboratory) **11-6,** pp. 1 – 11 (2011).

2.1. R. Sundaresan and J. O'M. Bockris, "Anomalous Reactions during Arcing between Carbon Rods in Water," *Fusion Technol.* **26**, 261 – 265 (1994).

2.2 M. Singh, M.D. Saksena, V.S. Dixit and V.B. Kartha, "Verification of the George Osawa Experiment for Anomalous Production of Iron from Carbon Arc in Water," *Fusion Technol.* **26**, 266 – 270 (1994).

2.3 I. Ogura, I. Awata, T. Takigawa, K. Nakamura, O. Horibe and T. Koga, "On the Carbon Arc Discharge in Water," *Chemistry Express* **7**, pp. 257 – 260 (1992) (in Japanese).

2.4 T. Hanawa, "X-ray Spectrometric Analysis of Carbon-Arc Products in Water and Alkali Carbonate Solution, "*Abstracts of JCF1*, page 12 (1999) (in Japanese). And also T. Hanawa, "X-ray spectrometric Analysis of Carbon Arc Products in Water," *Proc. ICCF8*, pp. 147 – 152 (2000). ISBN 88-7794-256-8.

2.5 E. Esko, "Production of Metals from Non-Metallic Graphite," *Infinite Energy* **78**, pp. 42 – 43 (2008)

2.6 R. Takahashi, "Synthesis of Substance and Generation of Heat in Charcoal Cathode in Electrolysis of H_2O and D_2O using Various Alkali hydroxides," *Proc. ICCF5*, pp. 619 – 622 (1995). And also R. Takahashi, "Anomalous Increase in Excess Heat in Electrolysis of Heavy Water and Light Water for Use of Drilled Cathode of Charcoal," *Proc. ICCF6*, pp. 546 – 550 (1996).

2.7 Suess and Urey, "Abundances of the Elements" *Rev. Mod. Phys.* **28**, pp. 53 – 74 (1956).

2.8 H. Kozima, "Elemental Transmutation in Biological and Chemical Systems", *Cold*

Fusion 16, 30 – 32 (1996).
2.9 H. Kozima, *Discovery of the Cold Fusion Phenomenon*, Ohtake Shuppan, 1998. ISBN 4-87186-044-2.

3.1 B. Jonson, "Light Dripline Nuclei," *Phys. Rep*. **389**, pp. 1 – 59 (2004)
3.2 K. Tanaka, T. Suzuki et al., "Observation of a Large Reaction Cross Section in the Drip-Line Nucleus ^{22}C," P*hys. Rev. Lett.* **104**, pp. 062701 – 062704 (2010)
3.3 T. Nakamura, N. Kobayashi et al., "Halo Structure of the Island of Inversion Nucleus ^{31}Ne," *Phys. Rev. Lett.* **103**, pp. 262501 – 262504 (2009).
3.4 A.S. Jensen, K. Riisager, D.V. Fedorov and E. Garrido, "Structure and Reactions of Quantum Halos," *Rev. Mod. Phys.* **76**, pp. 215 – 261 (2004).
3.5 S. Patchkovskii, J.S. Tse, S.N. Yurchenko, L. Zhechkov, T. Heine and G. Seifert, "Graphene nanostructures as tunable storage media for molecular hydrogen," *Proc. National Academy of Science*, **102**, pp. 10439 – 10444 (2005).
3.6 K. Fukuda, T. Umeno and Y. Hara, "*Natural Graphite/Carbon Composite Anode Material as Lithium Ion Battery*," *Materials Integration* **17**, No.1, pp. 45 – 50 (2004) (in Japanese).
3.7 K.R. Kganyago and P.E. Ngoepe, "Structural and electronic properties of lithium intercalated graphite LiC_6," *Phys. Rev.* **B 68**, 205111- 205126 (2003)
3.8 G. Majer, E. Stanik and S. Orimo, "NMR studies of hydrogen motion in nanostructured hydrogen-graphite systems" *Journal of alloys and compounds* Vol. 356-57, 617 – 621 (2003).
3.9 S. Chiu and A.A. Haasz, "Hydrogen Transport and Trapping in Graphite**,"** *UTIAS Report* No. 347, Institute for Aerospace Studies, Univ. Toronto, 1994. CN ISSN 0082-5255.

4.1 V.I. Vysotskii, A.A. Kornilova and A.B. Tashyrev, "Investigation of Memory Phenomena in Water and Study of Isotopes Transmutation in Growing Biological Systems Containing Activated Water," *Proc. ICCF13*, pp. 477 – 497 (2007).
4.2 N. Inami, M.A. Mohamed, E. Shikoh and A. Fujiwara, "Synthesis-condition dependence of carbon nanotube growth by alcohol catalytic chemical vapor deposition method" *Science and Technology of Advanced Materials*, **8**, pp. 292–295 (2007).